Article
Chinese Science Bulletin
Progress of Projects Supported by NSFC
Materials Chemistry
November 2012 Vol.57 No.31: 4019–4023
doi: 10.1007/s11434-012-5363-0

Porous cobalt oxide nanowires: Notable improved gas sensing performances

MA MaiXia[1,5], PAN ZhiYun[2], GUO Lin[1*], LI JingHong[3], WU ZiYu[2] & YANG ShiHe[1,4]

[1] *School of Chemistry and Environment, Beijing University of Aeronautics and Astronautics, Beijing 100191, China;*
[2] *National Synchrotron Radiation Facility, University of Science and Technology of China, Hefei 230026, China;*
[3] *Department of Chemistry, Beijing Key Laboratory for Microanalytical Methods and Instrumentation, Key Laboratory of Bioorganic Phosphorus Chemistry & Chemical Biology, Tsinghua University, Beijing 100084, China;*
[4] *Department of Chemistry, the Hong Kong University of Science and Technology, Clear Water Bay, Kowloon, Hong Kong, China;*
[5] *Faculty of Chemistry and Material Science, Langfang Teachers College, Langfang 065000, China*

Received March 7, 2012; accepted May 23, 2012

The porous Co_3O_4 nanowires have been successfully synthesized via modified template method. A possible growth mechanism governing the formation of such 1D nanowires is proposed. The as-prepared products have been characterized by X-ray Powder Diffraction (XRD), Extended X-ray Absorption Fine-structure (EXAFS), High-resolution Transmission Electron Microscopy (HRTEM) and N_2 adsorption/desorption analysis. Our systematic studies have revealed that the porous Co_3O_4 nanowires show excellent gas sensing performances, which demonstrate the potential application of the 1D nanostructured Co_3O_4 in the detection of the ethanol gas as a sensor material. The improved performances are owing to its large specific surface area and porous morphology.

nanostructures, cobalt oxides, XAFS, gas sensors

Citation: Ma M X, Pan Z Y, Guo L, et al. Porous cobalt oxide nanowires: Notable improved gas sensing performances. Chin Sci Bull, 2012, 57: 4019–4023, doi: 10.1007/s11434-012-5363-0

Transition-metal oxides with controlled nanostructures, such as nanotubes or nanowires, have peculiar properties and potential applications in a way distinct from their bulk counterparts because such nanostructuring may have a profound influence on the properites of these materials [1–3]. Cobalt oxide (Co_3O_4) based nanostructures have attracted great interest in the past few years. Recently, various morphologies of Co_3O_4 nanostructures have been prepared [4–7]. In particular, the thermal conversion of cobalt nitrate hexahydrate in silica templates to nanowires has proven to be promising. Thus, it is worthwhile to study the gas-sensing characteristics of one-dimensional (1D) Co_3O_4 nanowires. The extended X-ray absorption fine-structure (EXAFS) technique is a powerful tool for probing the local atomic structures because of its element specificity and independence of the long-range order of materials [8]. The EXAFS spectra have provided many quantitative structural parameters such as interatomic distance, co-ordination number, and Debye-Waller factor [9]. EXAFS study is an indispensable method for investigate the local structure in the interior and at the surface, as well as bonding information of a variety of solid-state materials [10].

Herein, we report on a template synthesis leading to porous Co_3O_4 nanowires using SBA-15 as hard templates. Moreover, the local structure in the interior and at the surface of the Co_3O_4 nanowires and the bulk Co_3O_4 were studied by EXAFS. The gas-sensing application of the as- prepared porous Co_3O_4 nanowires was systematically investigated in detail.

1 Experimental

All the chemical reagents used in the experiment are

*Corresponding author (email: guolin@buaa.edu.cn)

analytical grade. The total synthesis includes two steps. In the first step, the mesoporous silicas, two-dimensional (2D) hexagonal SBA-15 were synthesized according to ref. [11]. In the second step, the Co_3O_4 nanowires were synthesized by using SBA-15 as hard templates. During the experiment, 0.5 g of SBA-15 and 1 g of cobalt nitrate hexahydrate ($Co(NO_3)\cdot 6H_2O$, 98%, Alfa Aesar) were first dissolved in 20 mL ethanol at room temperature by intensive magnetic stirring for 2 h to obtain a homogeneous pink solution. The ethanol was then evaporated off at approximately 60°C. During the process, the cobalt nitrate was drawn into the pores by capillary action. The dry sample was then thermally decomposed at 300°C for 1 h and 500°C for 3 h. The SBA-15 silica template was removed by a 10% solution of HF. Afterward, the final precipitate was collected by filtration and washed with ethanol and distilled water for several times, and then dried at 60°C to obtain the dark powders. To compare the performance of gas sensing, commercial Co_3O_4 (99.7%) were purchased from Alfa Aesar Company.

The samples were characterized by X-ray powder diffraction (XRD) using a Rigaku Dmax2200 X-ray diffractometer with Cu Kα radiation (λ=0.15416 nm). Transmission electron microscopy (TEM) and high-resolution TEM (HRTEM) investigations were performed using a JEOL JEM-2100F microscope. Brunauer-Emmett-Teller (BET) nitrogen-adsorption-desorption was measured by using NOVA-2200e Surface Area and pore size Analyzer (Quantachrome instruments). The Co K-edge XAFS spectra of porous Co_3O_4 nanowires and bulk Co_3O_4 were measured at the U7C beamline of National Synchrotron Radiation Laboratory (NSRL), China. The storage ring of NSRL was run at 0.8 GeV with a maximum current of 250 mA. A double crystal Si (111) monochromator was used as a monochromator. The XAFS signals were collected in transmission mode at room temperature. XAFS data were analyzed by UWXAFS3.0 [12] and USTCXAFS3.0 [13] software packages according to the standard data analysis procedures.

Gas-sensing properties were measured using a static system controlled by a computer according to the literature [14].

2 Results and discussion

2.1 Synthesis and characterization of the porous Co_3O_4 nanowires

A simple modified template method was employed to synthesize the porous Co_3O_4 nanowires. The powder XRD patterns of the obtained products are showed in Figure 1. From the Figure 1, all the diffraction peaks of the two samples can correspond to a pure cubic phase of Co_3O_4 with lattice parameters of a=b=c=0.8084 nm according to JCPDS card No. 43-1003. We can see that the peak intensity and broadening of two samples are different. The peak intensity of the bulk (Figure 1(a)) is stronger, indicative of highly crystallinity.

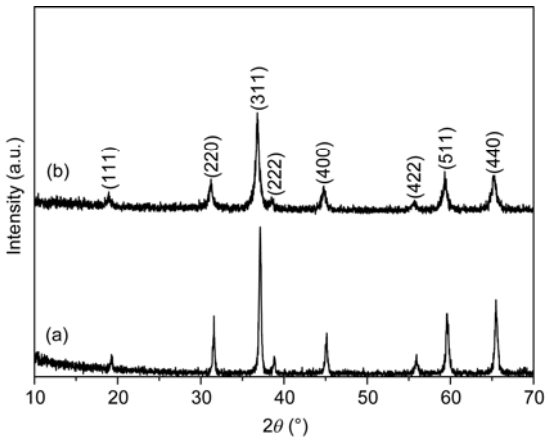

Figure 1 XRD patterns of (a) bulk Co_3O_4 and (b) porous Co_3O_4 nanowires.

The obvious peak broadening of the nanowires (Figure 1(b)) can be attributed to the small size effect and mesoporous morphology produced in the decomposition.

Figure 2 shows the XAFS signal in R space of the bulk Co_3O_4 and Co_3O_4 nanowires. We all know that Co_3O_4 consists of one third Co^{2+} ions and two thirds Co^{3+} ions. In Figure 2, the first peak at about 1.5 Å is due to the Co(II,III)-O coordination in the first shell, the second peak at about 2.8 Å corresponds to the Co(III)-Co(III), Co(II)-Co(II) and Co(II)-O coordination in the second shell. From Figure 2, we note that the peak intensity of Co_3O_4 nanowires is weaker than that of the bulk Co_3O_4, which demostrates disorder degree increases. These changes are essentially attributed to the influences of a surface layer with different composition and electronic structure from the bulk material [15]. It further indicates that electronic structures in materials with a smaller free surface and within a nanometer scale probably differs from that in the corresponding bulk material [15].

Table 1 summarizes the curve-fitting results of the EXAFS spectra. Compared with bulk Co_3O_4, the DW factor of

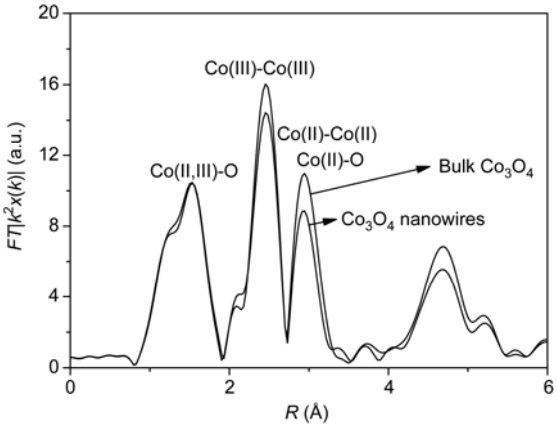

Figure 2 The radial structure functions of the Co_3O_4 nanowires and bulk Co_3O_4. XAFS signal in R space for the Co_3O_4 nanowires and bulk Co_3O_4.

Table 1 Fitting results of the coordination numbers and bond lengths for the first and the second shells in the Co_3O_4 nanowires and bulk Co_3O_4

Samples	Bond	R(Å)[a]	N[b]	ΔE[c]	$\sigma^2(10^{-3}Å^2)$[d]
Co_3O_4 Nanowires	Co(II)–O	1.85±0.01	4	–8.1±3.0	1.8±1.2
	Co(II)–Co(II)	3.33±0.02	12	–8.1±3.0	4.3±1.0
	Co(II)–O	3.36±0.02	12	–8.1±3.0	4.3±1.0
	Co(III)–O	1.92±0.01	6	–9.4±2.6	1.8±1.2
	Co(III)–Co(III)	2.84±0.02	6	–9.4±2.6	4.3±1.0
Bulk Co_3O_4	Co(II)–O	1.85±0.01	4	–5.9±1.4	3.3±1.3
	Co(II)–Co(II)	3.34±0.01	12	–5.9±2.5	3.4±1.0
	Co(II)–O	3.37±0.02	12	–5.9±2.5	3.4±1.0
	Co(III)–O	1.93±0.01	6	–6.2±1.4	3.3±1.3
	Co(III)–Co(III)	2.85±0.02	6	–6.2±2.5	3.4±1.0

a) R is the bond length; b) N is the coordination number; c) ΔE is the shift of energy threshold; d) σ^2 is the Debye-Waller factor.

Co_3O_4 nanowires is smaller in the first coordination shells. However, the DW factor of Co_3O_4 nanowires is much larger than that of bulk Co_3O_4 in the second coordination shells. It illustrates thermal energy and structural disorder in the second coordination shells increase when Co_3O_4 become the 1D nanostructure. The shift of energy threshold (ΔE) of nanowires is much larger than the bulk Co_3O_4, which demostrates Co_3O_4 nanowires have more active sites than the bulk Co_3O_4. The Debye-Waller (DW) factor σ^2 from EXAFS represents the fluctuation of relative positions between the absorbing and scattering atoms [16]. From the Table 1, we also note that the Co–O bond length of the nanowires is slightly shorter than that of the bulk Co_3O_4, indicative of a structural contraction for the nanowires, which demonstrates that the interaction between oxygen (or cobalt) and cobalt is stronger in these 1D Co_3O_4 nanowires samples than in the bulk Co_3O_4. These results agree well with the results observed in gas sensing applications.

The crystalline structure of the Co_3O_4 nanowires were analysed by TEM and HRTEM in Figure 3. From Figure 3(a), it can be seen that this morphology dominates throughout the material. The symmetry of the mesostructures are the same as the symmetry of the porous silicon dioxide, space groups P6mm for the nanowires. From Figure 3(b), it is obvious that the samples are composed of nanowires with an average diameter of 7–11 nm and the length reach to about 200 nm. As shown in Figure 3(c), the more-ordered pores of Co_3O_4 nanowires show a narrow distribution around 4 nm. The nanowires are single crystals showing the planes of (311) with the spacing of 0.24 nm (Figure 3(d)).

The formation of the pores may be attributed to the impact of gas evolution during the thermal decomposition reaction. Figure 4 shows the N_2 adsorption-desorption isotherms and BJH pore size distribution plots of the samples prepared by using SBA-15 as hard template. The Brunauer-Emmett-Teller (BET) surface area of the Co_3O_4 nanowires was determined to be 81.63 $m^2\ g^{-1}$. This curve shows type IV isotherms with an H1 hysteresis loop according to the classification of adsorption isotherms and adsorption hysteresis loop [17], confirming the mesoporosity. These

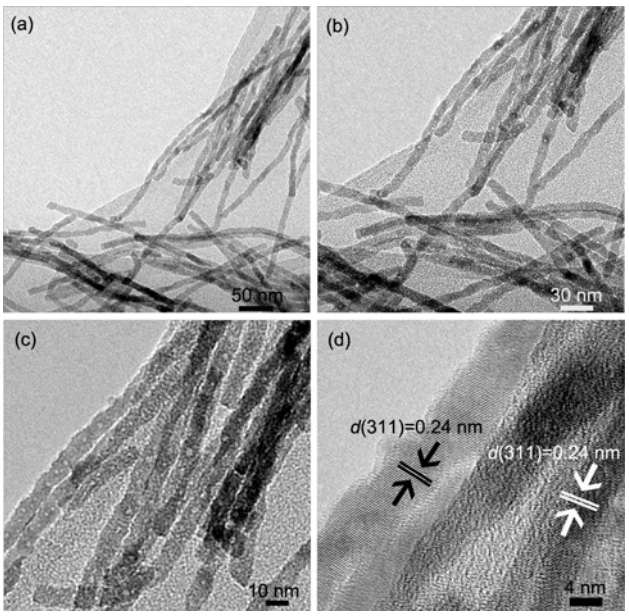

Figure 3 (a), (b) and (c) TEM images of the porous Co_3O_4 nanowires in a direction perpendicular to the wires and (d) corresponding high resolution image.

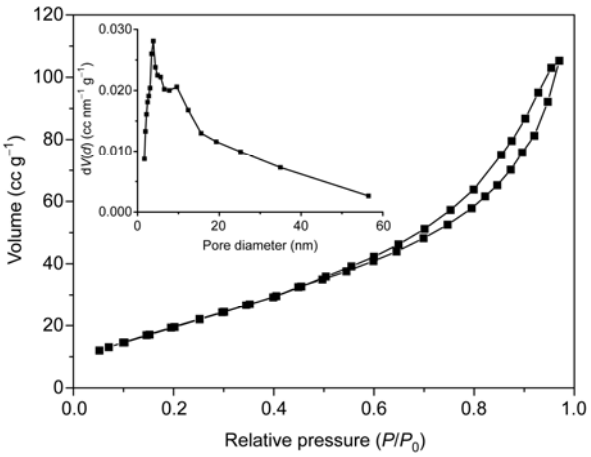

Figure 4 N_2 adsorption/desorption isotherms and the pore size distributions of the porous Co_3O_4 nanowires.

mesopores were produced from the removal of pore wall of SiO_2 hard template.

Figure 5 shows schematic diagram of the preparation of porous Co_3O_4 nanowires. Porous Co_3O_4 nanowires were synthesized by using the following three steps. (1) Impregnation. The cobalt nitrate was drawn into the pores by capillary action. (2) Calcination. The poisonous gases were introduced into a glass container filled with sodium hydroxide solution so that the harmful gases can be absorbed so as not to pollute the air. Through the thermal decomposition, the product was cooled to room temperature; the color was changed from pink to black, signifying the formation of cobalt oxide. (3) Template dissolution. To obtain self-

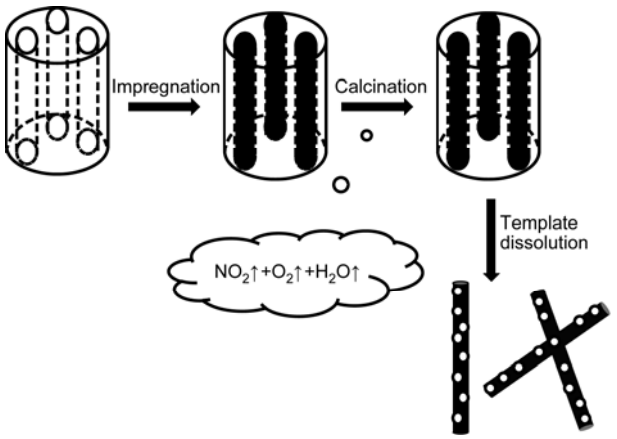

Figure 5 Schematic diagram showing the preparation of the porous Co_3O_4 nanowires.

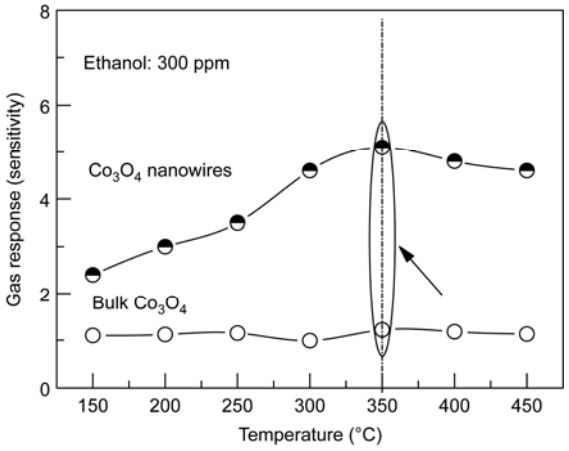

Figure 6 Sensitivity response of the gas sensors for the Co_3O_4 nanowires and bulk Co_3O_4 vs operating temperature from 150 to 450°C.

sustained nanowires, the product was dissolved in 10% HF. The possible reactions involved of the three steps can be described as

porous nanowires preparation:

$$3Co(NO_3)_2\cdot 6H_2O\rightarrow Co_3O_4+6NO_2\uparrow+O_2\uparrow+6H_2O\uparrow$$

NO_2 absorption:

$$2NO_2+2NaOH\rightarrow NaNO_3+NaNO_2+H_2O$$

template dissolution:

$$SiO_2+4HF\rightarrow SiF_4\uparrow+2H_2O$$

2.2 Application in gas sensors

The important application of the Co_3O_4 is the functional role as a gas sensing materials for detection of some gas molecules. Here, the semiconducting nanowires were used as the sensors material to detect the C_2H_5OH gas.

The sensitivity of the obtained porous Co_3O_4 nanowires and the bulk Co_3O_4 to C_2H_5OH gas with a concentration of 300 ppm under various operating temperature are showed in Figure 6. We can see that the sensor response increases at an initial stage but decreases afterwards with the continuing rise of temperature, thereby passing through a zenith at 350°C. This can be explained qualitatively from a dynamic balance between initial fast adsorption of ethanol molecule and the further acceleration of desorption, as the temperature maintains rising [18]. Moreover, this can also be understood by considering the other possibility: the reaction rate between the ethanol and the sensing material increases as temperatures increases to the optimal value, and further decrease of sensor response after the optimum can be ascribed to the reduced gas concentration due to the combustion of the tested gas [19]. Compared with the nanowires sensors, the bulk sensors have less active sites and less surface area, which enable the detecting gases to access less surfaces. So the change of reaction rate between the ethanol and the bulk sensing material is slow with the continuing rise of temperature. From Figure 6, we also note that the porous Co_3O_4 nanowires exhibits superior gas-sensing capabilities towards C_2H_5OH than the bulk Co_3O_4. The highest sensitivity of Co_3O_4 nanowires is estimated to be 5.1 and much higher than that of the bulk Co_3O_4 (less than 4). Evidently, the Co_3O_4 nanowires is a potential material for detecting ethanol. According to the ref. [20], the change of resistance in Co_3O_4 sensors is mainly caused by the adsorption and desorption of gas molecules on the surface of the sensing structure. Figure 7 shows typical response-recovery characteristics for the porous Co_3O_4 nanowires and bulk Co_3O_4 sensor under C_2H_5OH gas concentration of 300 ppm. From the curve of Co_3O_4 nanowires, we can see that the voltage increases abruptly when the C_2H_5OH gas is introduced, however, the voltage returns to original state when the ethanol gas is released. The curve of bulk Co_3O_4 is different from the nanowires, which indicates the strong dependence of response and recovery time on the 1D nanostructure.

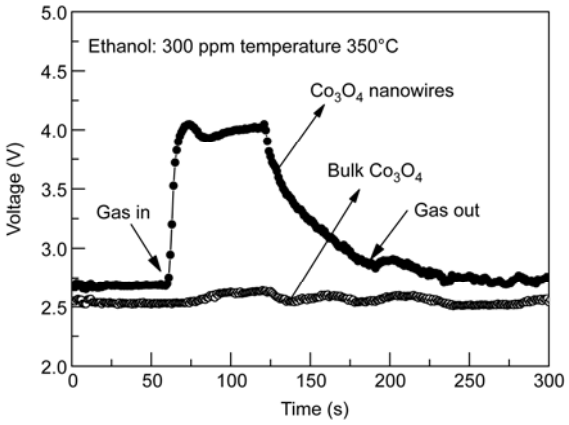

Figure 7 Response-recovery characteristics for Co_3O_4 nanowires and bulk Co_3O_4 sensors to C_2H_5OH gas operated at 350°C. The C_2H_5OH gas concentration is fixed at 300 ppm.

3 Conclusions

To summarize, the porous Co_3O_4 single crystals nanowires with diameter about 7–11 nm and length about 200 nm have been synthesized via template method. Moreover, gas-sensing testing of the porous Co_3O_4 nanowires indicates the excellent sensitivity to alcohol. These results show that the porous Co_3O_4 nanowires are attractive for application in gas sensors, which may open up an avenue for effectively tuning gas sensing character of the 1D nanostructured Co_3O_4.

This work was supported by the National Natural Science Foundation of China (11079002,20973019), and Specialized Research Fund for the Doctoral Program of Higher Education (20091102110035).

1 Patzke G R, Krumeich F, Nesper R. Oxidic nanotubes and nanorods-anisotropic modules for a future nanotechnology. Angew Chem Int Ed, 2002, 41: 2446–2461
2 Tenne R. Advances in the synthesis of inorganic nanotubes and fullerene-like nanoparticles. Angew Chem Int Ed, 2003, 42: 5124–5132
3 Hou Z Y, Li G G, Lian H Z, et al. One-dimensional luminescent materials derived from the electrospinning process: Preparation, characteristics and application. J Mater Chem, 2012, 22: 5254–5276
4 Varghese B, Zhang Y S, Dai L, et al. Structure-mechanical property of individual cobalt oxide nanowires. Nano Lett, 2008, 8: 3226–3232
5 He T, Chen D R, Jiao X L, et al. Surfactant-assisted solvothermal synthesis of Co_3O_4 hollow spheres with oriented-aggregation nanostructures and tunable particle. Langmuir, 2004, 20: 8404–8408
6 Li T, Yang S G, Huang L S, et al. A novel process from cobalt nanowire to Co_3O_4 nanotube. Nanotechnology, 2004, 15: 1479–1482
7 Feng J, Zeng H C. Size-controlled growth of Co_3O_4 nanotubes. Chem Mater, 2003, 15: 2829–2835
8 Wu Z H, Guo L, Li Q S, et al. Surface atomic structures of Fe_2O_3 nanoparticles coated with cetyltrimethyl ammonium bromide and sodium dodecyl benzene sulphonate: An extended X-ray absorption fine-structure study. J Phys: Condens Matter, 1999, 11: 4961–4970
9 Min G K, Jaephil C. Reversible and high-capacity nanostructured electrode materials for Li-ion batteries. Adv Funct Mater, 2009, 19: 1497–1514
10 Guo L, Liu C M, Wang R M, et al. Large-scale synthesis of uniform nanotubes of a nickel complex by a solution chemical route. J Am Chem Soc, 2004, 126: 4530–4531
11 Zhao D Y, Huo Q S, Feng J L, et al. Nonionic triblock and star diblock copolymer and oligomeric surfactant syntheses of highly ordered, hydrothermally stable, mesoporous silica structures. J Am Chem Soc, 1998, 120: 6024–6036
12 Stern E A, Newville M, Ravel B, et al. The UWXAFS analysis package: Philosophy and details. Physica B, 1995, 208: 117–120
13 Zhong W J, Wei S Q. USTCXAFS 2.0 Software Package. J Chin Univ Sci Technol, 2001, 31: 328–333
14 Zeng W, Liu T M, Wang Z C, et al. Selective detection of formaldehyde gas using a Cd-doped TiO_2-SnO_2 sensor. Sensors, 2009, 9: 9029–9038
15 Zhang Z L. Surface effects in the energy loss near edge structure of different cobalt oxides. Ultramicroscopy, 2007, 107: 598–603
16 Matsuura M, Asada K, Konno K, et al. EXAFS debye-waller factors of La and Ni in $LaNi_5$. J Alloys Comp, 2005, 390: 31–34
17 Sing K S W, Everett D H, Haul R A W, et al. Physical and biophysical chemistry division commission on colloid and surface chemistry including catalysis. Pure Appl Chem, 1985, 57: 603–619
18 Xu J Q, Jia X H, Lou X D, et al. Selective detection of HCHO gas using mixed oxides of ZnO/$ZnSnO_3$. Sens Actuators B, 2007, 120: 694–699
19 Sakai G, Matsunaga N, Shimanoe K, et al. Theory of gas-diffusion controlled sensitivity for thin film semiconductor gas sensor. Sens Actuators B, 2001, 80: 125–131
20 Li W Y, Xu L N, Chen J. Co_3O_4 nanomaterials in lithium-ion batteries and gas sensors. Adv Funct Mater, 2005, 15: 851–857